Physical Parameter Estimation in rock samples via Image Analysis of Computed Micro-Tomographies (CMT)

Andres Medina*, Doug Schimtt, Randy Koffman, and Gautier Njiekak. University of Alberta, Edmonton, Alberta, Canada.

aamedina@aulberta.ca

Summary

Digital image processing techniques are used for estimating total porosity and pore perimeter directly from rock sample images obtained through CMT scanning. Furthermore, permeability estimation is attained, indirectly, by using these two physical parameter estimates in the Kozeny-Carman equation.

The proposed image processing procedure is tested in x-ray CMT scans of sedimentary rocks (carbonates) and results for total porosity estimates are contrasted with Hg-intrusion and He-pycnometry porosity measurements. Also, Kozeny-Carman permeability estimations are compared with air-permeability measurements.

Introduction

Image processing is used as an assessment tool for rock sample physical parameter measurements, (*Arns et al.*, 2002), (*Kameda and Dvorkin,* 2004). It allows analysis of rock physical parameters at different scales in a non-invasive way. Constrained by image resolution, regions of interest such as compositional material inside the rock matrix or pore space can be detected in CMT-scans. Here, pore space and rock matrix separation is performed by means of image segmentation; therefore, total porosity can be estimated directly from segmented images.

Kozeny-Carman permeability estimates are achieved indirectly using total porosity and previously estimated *specific surface* of the samples, i.e. the ratio of the pore surface area and the volume of the sample. Pore surface area estimation is obtained by pore-edge extraction of the CMT scans.

Theory and/or Method

In an appropriate rock sample CMT-scan, total porosity is estimated using a segmented version of the CMT-scan, by means of:

$$\hat{\phi}_T = \frac{A_p}{A_T}, \tag{1}$$

where A_p is the pore space area in the segmented image and A_T the total area of the rock matrix. Due to adimensionality and pixel resolution, equation (1) is rewritten in terms of pixel count as:

$$\hat{\phi}_T = \frac{P_0}{P_T}, \tag{2}$$

where P_0 is the pore space pixel count and P_T the total number of pixels.

The original gray-scale CMT-scans are transformed into binary images by mapping the rock correspondent gray-intensities to a value of one and the rest to zero. This implies selection of an appropriate gray-intensity threshold value. Here, a CMT-scan dependent threshold is implemented. The adaptive threshold is selected from a continuous version of the function of each CMT-scan histogram, as the minimum of the saddle points of such function. This threshold criterion is based on the idea that histograms for a collection of CMT-scans for a rock sample are expected to have the same shape. Let f be the continuous version of a CMT-scan histogram, then:

$$\tilde{s} := \min\{s \in [0, 255] |\, \partial^2 f / \partial s = 0\}, \text{ and} \tag{3}$$

$$\tau(s) = \delta(s > \tilde{s}), \tag{4}$$

defines the segmentation performed in each gray-intensity CMT-scan. In equation (4), $\delta(A) = 1$, when condition A is satisfied and $\delta(A) = 0$, otherwise.

After each CMT-scan is segmented, pore edge detection is performed. The specific procedure used is based on the *discrete wavelet transform* (DWT) and the *morphological opening* of each CMT-scan. Morphological opening of an image reduces edge-bumps and other noise related artifacts that might appear after segmentation (*Gonzalez et al.,* 2009), thus smoothing the pore contour of a CMT-scan. DWT is applied to the *opened* image, in the DWT domain: the *approximation coefficients* are mapped to zero and then an inverse DWT is applied, thus pore edges are retrieved and pixel count is performed.

Let L_p be the pore perimeter of a processed CMT-scan, then, specific surface, as a measure of the ratio of pore space surface area, can be approximated (*Rink and Schoper, 1978*), by:

$$S_s = \frac{4}{\pi}\frac{L_p}{A_p}. \quad (5)$$

Total porosity estimates provides information only on the general amount of pore volume in a rock sample, whilst specific surface reckons for how fine pores can be.

Assuming an intrinsic interconnectedness of the pore space system, permeability can be related to porosity through the Kozeny-Carman equation (*Costa*, 2006). Here, a version by (*Ruzyla*, 1986) is used:

$$\kappa_{ck} = \frac{\phi^3}{5(1-\phi^2)S_s^2} = \frac{A_f^3}{5\left(1-A_f^2\right)(4/\pi(P/A_t))^2}, \quad (6)$$

where A_f is the area fraction of pore space.

Example

The method is applied to three different rock samples, A: a vuggy carbonate, B: an evaporite and C: a marly carbonate. Each sample had an approximate volume size of $(5 \times 5 \times 7)mm^3$. Images of the inner structure of these samples were obtained using an industrial x-ray CMT-scan, where the distance between consecutive CMT scans is $0.005mm$.

For each sample, every CMT-scan was cropped to avoid background interference. Threshold calculations by histogram processing were then performed; images were segmented by hard threshold using equation (4). Total porosity was calculated by using equation (2) and finally, these total porosity estimations were averaged to get a global estimate for each sample. Analogously, averages of specific surface were obtained and then used for Kozeny-Carman-permeability estimations.

Total porosity estimations for each sample are respectively $\widehat{\phi_A} = 3.12\%$, $\widehat{\phi_B} = 0.26\%$ and $\widehat{\phi_C} = 0.90\%$. Kozeny-Carman permeability estimations for each sample are: $\kappa_{KC_A} = 3.76 \times 10^{-12}cm^2$, $\kappa_{KC_B} = 2.57 \times 10^{-12}cm^2$, $\kappa_{KC_C} = 1.11 \times 10^{-12}cm^2$.

The same rocks were used for Hg-intrusion and He-pycnometry porosity measurements, although bigger sample sizes were used in these measurements. Results are summarized in Table 1.

Conclusions

Rock formation evaluation can be assessed using digital image processing methods for physical properties estimation. Some of the estimates can be achieved directly from the images as is the case of total porosity and specific surface and others indirectly as the Kozeny-Carman permeability. Agreement between direct measurements and estimation from the images is constrained by image resolution. The procedure can be applied independent of the scale at which the rock images were obtained or the image technique used.

This versatile method can be further explored to extend physical parameters and rock matrix characterization. In this case, pore space surface area was calculated, but this can be extended to characterize inner void space of a rock sample and separate void space due to fractures from the pore-related.

Acknowledgements

The author would like to thank Doug Schmitt, Gautier Njiekak and Randy Koffman for providing ideas, discussion and the CMT scans as well as the rock samples along with the data used in comparisons.

Sample	ϕ_{He}	ϕ_{Hg}	κ_{air}	$\bar{\phi}_T$	κ_{kc}
A	4 %	3 %	<2 mD	3.12 %	0.40 mD
B	3 %	4 %	<2 mD	0.30 %	3e-8 mD
C	5 %	6 %	<2 mD	1.00 %	0.01 mD

Table 1: He/Hg-porosity and air intrusion permeability measurements and estimation results for total porosity and permeability using the proposed method.

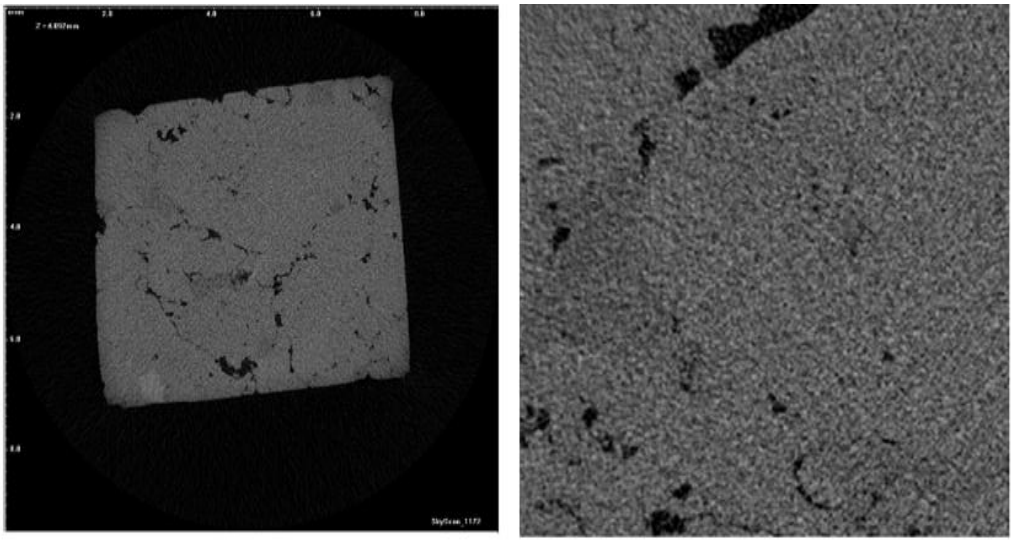

Figure 1: *Left:* Original CMT scan for sample A. *Right:* cropped CMT scan for segmentation.

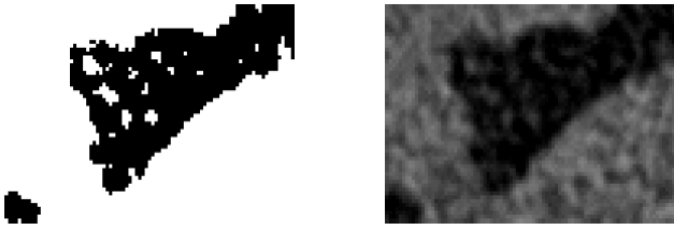

Figure 2: *Left:* Segmented CMT scan (detail). *Right:* Original CMT scan (detail).

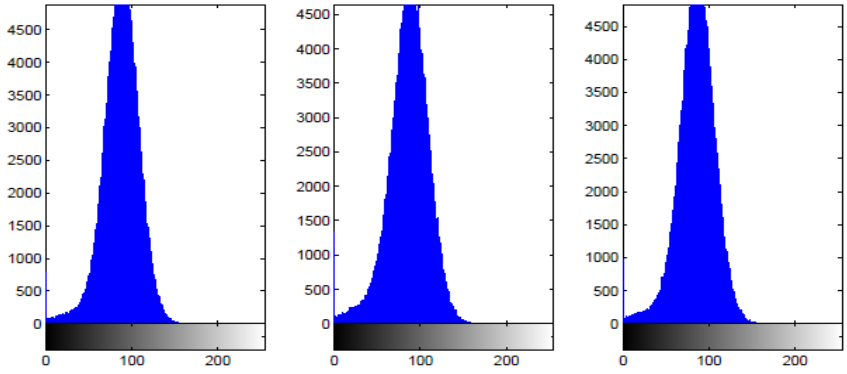

Figure 3: Histograms for three different CMT scans. The first inflection point is used as a threshold for image segmentation.

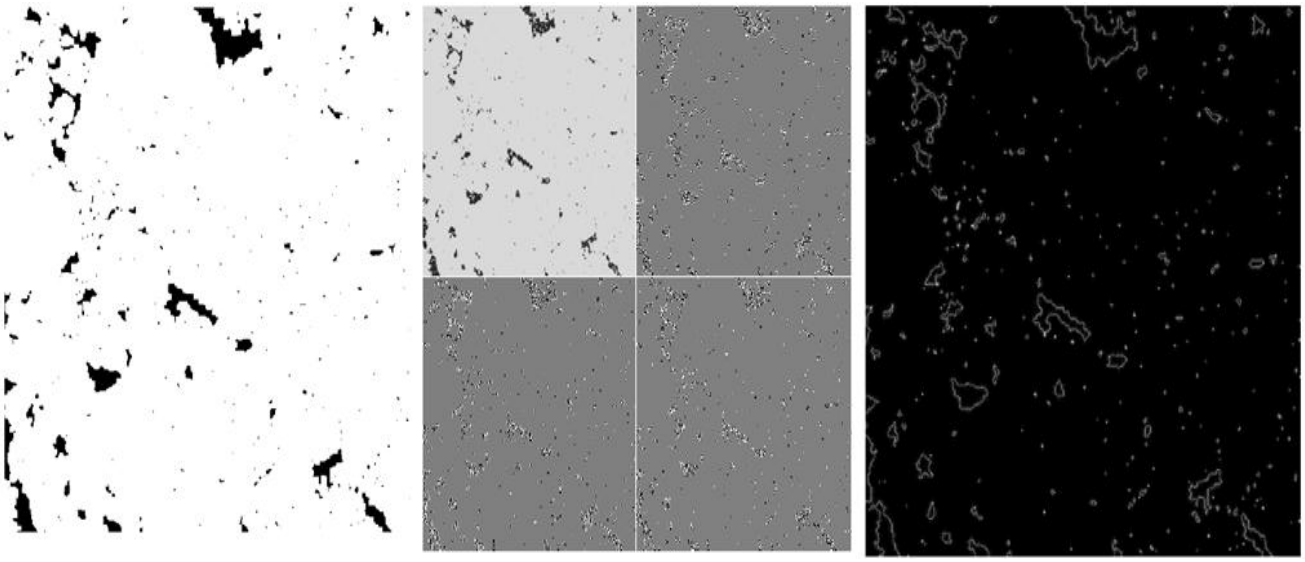

Figure 4: *Left:* Morphological opening. *Center:* DWT transform of the morphological opening. *Right:* Pore edge space after mapping scaling coefficients to zero.

References

Arns, C., Knackstedt, W. Pinczewski, W., and Garboczi, E., 2002. Computaion of linear elastic properties from microtomographic images: Methodology and agreement between theory and experiment. *Fire Research*, 67 (5).

Costa, A., 2006, Permeability-porosity relationship: A re-examination of the Kozenny-Carman equation based on a fractal pore-space geometry assumption*: Geophysical Research Letters*, 33.

Gonzalez R., Woods, R., and Eddins, S., 2009. Digital Image Processing using MATLAB, second ed., Gatesmack publishing.

Kameda, A., Dvorkin, J., 2004. To see a rock in a grain of sand: *The leading edge*, 23(8).

Rink, M.,and Schoper, J. 1978, On the application of image analysis to formation evaluation*, The Log Analyst*, XIX (1).

Ruzyla, K. 1986, Characterization of pore space by quantitative image analysis: *SPE Formation Evaluation*, 1(4).